Polish Society of Composite Materials
Polskie Towarzystwo Materiałów Kompozytowych

15: 3 (2015) 130-136

COMPOSITES THEORY AND PRACTICE

Patryk Nossol[1]*, Ralph Gliniorz[1,2], Lothar Kroll[1], Michael Heinrich[1,2]

[1] Technische Universität Chemnitz, Faculty of Mechanical Engineering, Department of Lightweight Structures and Polymer Technology, D-09107 Chemnitz, Germany
[2] Kompetenzzentrum Strukturleichtbau e.V. D-09126 Chemnitz
**Corresponding author: E-mail: patryk.nossol@mb.tu-chemnitz.de*

Received (*Otrzymano*) *3.02.2015*

APPLICATIONS OF MODAL ANALYSIS FOR EXAMINING STRUCTURAL STATE OF SYNTHETHIC-FIBRE NONWOVEN COMPOSITES

The dynamic behaviour of thermoplastic samples reinforced with aramid or polyester based nonwoven fabrics has been investigated. Changes in the structural state of specimens through open hole and impact damage could be proved by changes in modal parameters. Furthermore a directionality study has been performed showing clear dependence of modal parameters and fibre orientation. An appropriate frequency band was selected for a robust structural state detection of the samples. Additionally, a special modal hammer device was used to increase the accuracy of determining the modal parameters. This work continues investigations which can serve as a foundation for modal analysis based structural health monitoring (SHM) and quality control systems for composite structures.

Keywords: aramid nonwovens, polyester nonwovens, anisotropy, impact damage, open-hole, modal analysis, technical diagnostics, SHM, quality control system

ZASTOSOWANIE ANALIZY MODALNEJ DO BADANIA STANU STRUKTURY KOMPOZYTÓW WZMOCNIONYCH WŁÓKNINĄ SYNTETYCZNĄ

Zbadane zostało dynamiczne zachowanie próbek kompozytowych o osnowie termoplastycznej, wzmocnionych włókniną aramidową lub poliestrową. Wykazano, że zmiany w stanie struktury próbek, wywołane wierceniem otworów i uszkodzeniem udarowym, mogą być wykrywane w oparciu o zmiany parametrów modalnych. Przeprowadzono również badania, w których pokazano wyraźną zależność pomiędzy parametrami modalnymi a ukierunkowaniem włókien. Do właściwego wykrywania stanu strukturalnego próbek wybrane zostało odpowiednie pasmo częstotliwości. Dodatkowo zastosowane zostało specjalne urządzenie dla młotka modalnego zwiększające dokładność wyznaczania parametrów modalnych. Praca jest kontynuacją badań, które mogą służyć jako podstawa dla systemu przeznaczonego do monitorowania stanu konstrukcji oraz kontroli jakości, bazującego na analizie modalnej.

Słowa kluczowe: włóknina aramidowa, włóknina poliestrowa, anizotropia, uszkodzenia udarowe, otwory, analiza modalna, diagnostyka techniczna, monitorowanie stanu konstrukcji, kontrola jakości

INTRODUCTION

Research in vibration-based damage identification is constantly expanding. The basic idea behind this technology is that modal parameters are functions of the physical properties of the structure (mass, damping, and stiffness) [1]. Previously conducted investigations gave promising results shown in [2] for a modal analysis based structural health monitoring (SHM) system. In this work, further analysis is done with a focus on nonwoven fabric reinforced thermoplastics and improved measurement accuracy where similar results are expected as presented in [2]. The used composites are created using nonwoven fabrics with synthetic polyethylene terephthalate (PET) fibres or aramid fibres (AF) and a thermoplastic polypropylene (PP) matrix. Nonwoven fabrics often have specific properties that are high performance ready for a wide range of applications. These properties can be achieved by selecting certain materials and technologies which is presented in [3]. In particular, thermoplastic nonwovens offer ideal compatibility with thermoplastic matrix systems. That makes them ideal for high-volume production with high efficiency in costs and energy. Aramid fibre reinforced composites due to their high strength and very high resistance to crack propagation are highly desirable. For these reasons aramid fibres are used in impact-loaded laminates [4]. Additionally, nonwoven composites also offer the possibility to integrate a new generation of sensors and isolate conductor tracks (like those presented in [5, 6]) which make them interesting for SHM-Systems.

MATERIALS AND SAMPLE PREPARATION

The investigated plates in this work consist of alternating layers: nonwovens (PET UD/ISO 100 g/m² or AF 65 g/m²) and thermoplastic foils (PP, thickness: 200 μm), also known as organic sheets [7]. All the nonwovens were produced by needle-punch technology from staple fibres.The PET fibre length is 80 mm and linear density is 3.3 dtex. The Aramid fibre length is 38 mm and linear density is 1.7 dtex. A symmetric composition (Fig. 1) and equal production direction (nonwovens) of the layers will ensure the mechanical properties of the used reinforcing nonwovens. The pursued fibre volume content amounts to 20% in each sample.

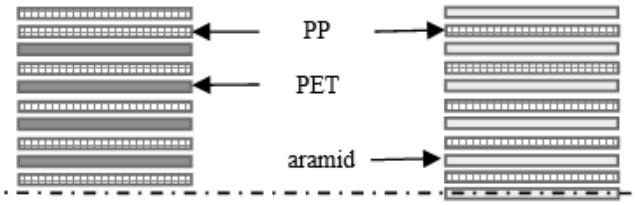

Fig. 1. Schematic representation of matrix/nonwoven symmetric composition

Rys. 1. Schematyczna budowa symetrycznego laminatu osnowa/włóknina

The production process of the organic sheets was realized in three steps: (1) cutting and stacking layers (300 mm x 650 mm), (2) putting the sheets between metal plates in a contact heating unit (4 bar, 220°C, 200÷370 s) with distance pieces (≈ 3 mm) and finally (3) consolidating them in an unheated (ambient temperature) press (500 kN, 80 s) until solidification. The temperature and holding time in the contact heating unit depend on the matrix material (PP) and thickness of each stack to ensure thorough heating for an optimally saturated matrix/nonwoven. Afterwards, all the samples were cut into squares (DIN EN ISO 6603-2 dimensions 140 mm x 140 mm) by water jet cutting. Three different types of material combinations were produced: PP matrix with a) PET-UD (unidirectional), b) PET-ISO (nearly isotropic features) and c) aramid. The average thickness of the organic sheets is 2.93 mm.

EXPERIMENTAL SET-UP

Modal analysis of samples

Measurement instrumentation

Similar to the investigations presented in [2], a modal hammer (Fig. 2-A) was used with an average of 5 hits per excitation point. Additionally, a special device was built to increase the accuracy of this excitation technique shown in (Fig. 2-B). A 3D joint tripod (Fig. 2-C) ensures precise positioning of the modal hammer head to the selected excitation point. To carry out the impulse using the device, it is sufficient to deflect and release the modal hammer, thanks to the built-in suspension system. The device ensures hitting the selected point with an almost constant angle to the surface, much more precisely than by hand. This excitation method is referred to as the "semi-automatic method". Similar to [2], the plates were examined in a frequency range from 0 to 5 kHz at 6 selected points (Fig. 3). The response was measured at point 6 with an uniaxial accelerometer (1 g) attached with beeswax, on the bottom of the structure as shown in Figure 2D.

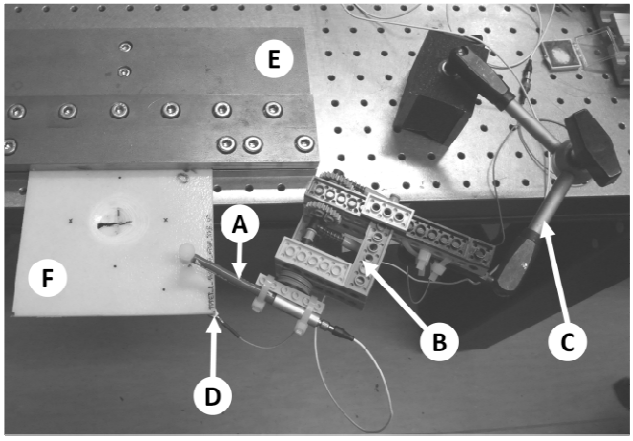

Fig. 2. Test stand (A - modal hammer; B - device to increase measurement accuracy; C - 3D joint tripod; D - accelerometer; E - clamping device; F - sample)

Rys. 2. Stanowisko badawcze (A - młotek modalny; B - urządzenie zwiększające dokładność pomiaru; C - statyw przegubowy; D - czujnik przyspieszenia; E - narzędzie mocujące; F - próbka)

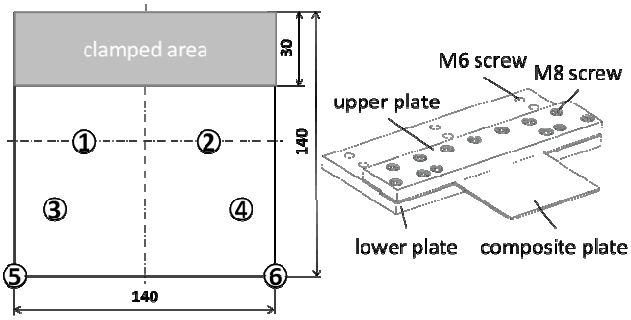

Fig. 3. Six selected points and clamping area for modal tests on organic sheet plates (left); used clamping device (right)

Rys. 3. Sześć wybranych punktów oraz mocowana powierzchnia do analizy modalnej (po lewej), narzędzie mocujące płyty (z prawej)

The same clamping device as in [2] was used (shown in Fig. 2-E and Fig. 3) to attach the composite plates (see, Fig. 2-F) accordingly. To avoid additional scattering of the modal parameters, a defined tightening torque of 20 Nm for all M6 and M8 screws was used (see [2] for more information).

Sensitivity study

Firstly, the influences of reattachment of the plates in the clamping device and the beeswax attached accelerometer on the measurement precision were examined. For that case, the scattering of the modal parameters was determined (see Table 1). Representative results for

the frequency response functions (FRFs) were provided by the excitation at the 3rd point (see FRFs $|H_{63}|$ in Figure 4).

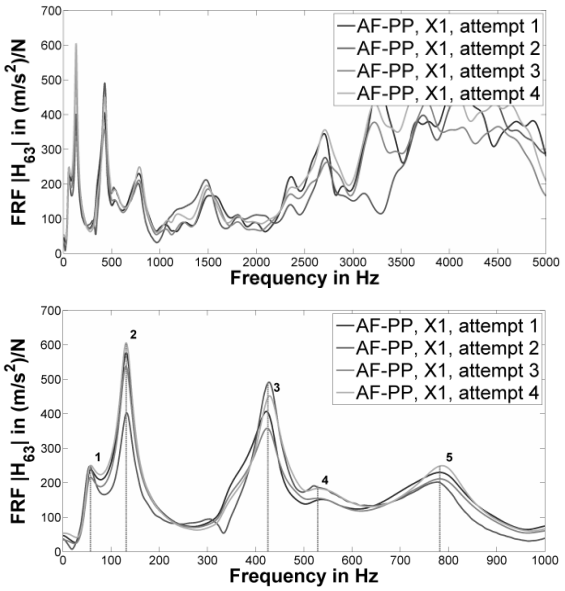

Fig. 4. Examination of influence of reattachment (AF-PP plate 1); till 5 kHz (upper); till 1 kHz (lower)

Rys. 4. Badanie wpływu ponownego mocowania (AF-PP plate 1); do 5 kHz (górny); do 1 kHz (dolny)

TABLE 1. **Scattering in first 5 modes of AF-PP plate 1**
TABELA 1. **Rozrzut w pierwszych 5 modach próbki AF-PP plate 1**

Mode	Standard deviation		
	Frequency [Hz]	Amplitude [(m/s²)/N]	Damping [%]
1	1.1	15.5	-
2	0.7	89.9	0.12
3	3.2	57.6	0.87
4	6.9	19.9	-
5	3.9	21.0	1.06

Investigations have been performed for the AF-PP plate 1 in the X1 direction by the semi-automatic method. Similar to [2], the plate was reattached in the clamping device four times with a new attachment of the accelerometer each time. The upper diagram in Figure 4 shows that scattering above ca. 1 kHz significantly rises. Therefore the frequency band for further analysis is limited to 1 kHz and offers 3-5 modes for a robust analysis of the nonwoven composites in terms of technical diagnostics. The calculated scattering in these investigations is further used to determine measurable changes in the modal parameters caused by fibre direction, impact damage and open holes.

Comparison of manual and semi-automatic excitation method

The next tests concern the influence of the excitation methods on the modal parameters and their reproducibility. Figure 5 shows the comparison between manual and semi-automatic determined FRFs. Table 2 demonstrates the standard deviation of the modal parameters in the four presented modes with a calculated ratio from (1) that indicates changes in measurement precision.

$$\text{ratio} = \frac{\text{SD manual}}{\text{SD semi - automatic}} \tag{1}$$

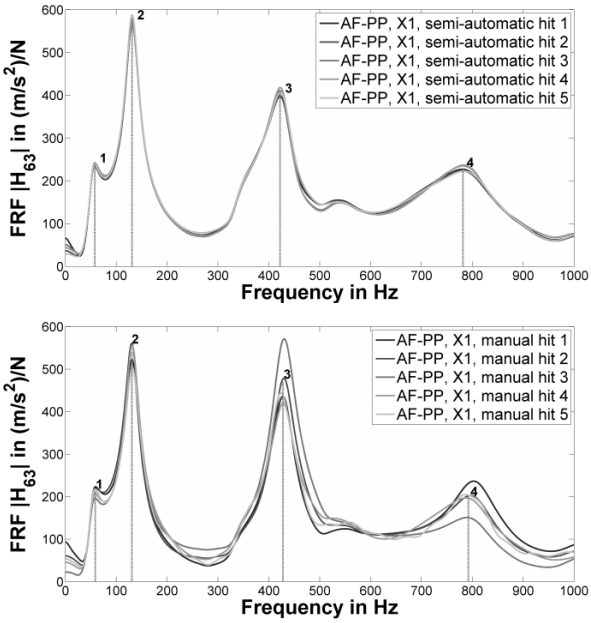

Fig. 5. Measurement accuracy of semi-automatic (upper) and manual (lower) excitation method; sample: AF-PP plate 1

Rys. 5. Dokładność pomiaru metodą półautomatyczną (górny) i manualną (dolny); próbka: AF-PP plate 1

TABLE 2. **Standard deviation (SD) in modal parameters and increase in measurement accuracy (ratio)**
TABELA 2. **Odchylenie standardowe (SD) parametrów modalnych oraz zwiększenie dokładności pomiaru (ratio)**

Mode	Frequency [Hz]		ratio
	SD semi-automatic	SD manual	
1	0.2	0.7	**3.5**
2	0.1	0.5	**5**
3	0.3	2.4	**8**
4	1.9	6.9	**3.6**
Mode	**Amplitude [(m/s²)/N]**		**ratio**
	SD semi-automatic	**SD manual**	
1	3.4	10.8	**3.2**
2	7.3	25.1	**3.4**
3	8.7	60.6	**7.0**
4	6.7	30.6	**4.6**
Mode	**Damping [%]**		**ratio**
	SD semi-automatic	**SD manual**	
1	-	-	-
2	0.04	0.46	**11.5**
3	0.32	0.35	**1.1**
4	0.88	1.09	**1.2**

Each FRF represents a single hit here. For the natural frequencies, both methods provide precise values.

The situation is different in determining the amplitudes of the mode shapes; the compared methods show a significant difference in measurement accuracy. In extreme cases (modal damping in 2nd mode), the semi-automatic method provides a standard deviation that is 11.5-times lower than that of the manual method. There is a significant increase in measurement precision; therefore these findings justify further use of the semi-automatic excitation method for all other investigations performed in this work.

Directionality study

Evaluation of the tensile test of the used nonwoven composites materials, 10 samples per material, in processing direction (x) and across (y), shows orthotropic properties (see Fig. 6). There are huge differences in the aramid nonwoven composites. For this reason, attempts have been made to investigate if this anisotropy can be detected in dynamical changes. This directional property results from the production process of the nonwoven fabrics. Because the plate layer compositions do not alternate the production direction of the nonwoven fabrics, it is possible to investigate this anisotropy by attaching and analyzing each plate in two perpendicular directions (X1, Y1) with the same grid of excitation points as shown in Figure 7.

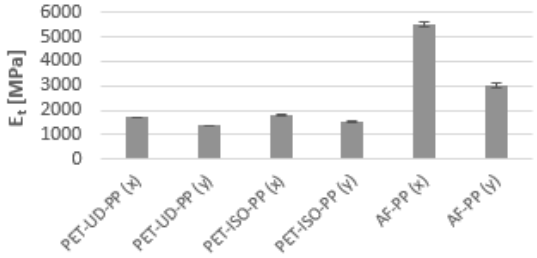

Fig. 6. Average values for Young's modulus from tensile test (E_t) in processing direction (x) and across (y)

Rys. 6. Średnie wartości modułu Younga z prób rozciągania (E_t) w kierunku wytwarzania (x) i poprzecznie (y)

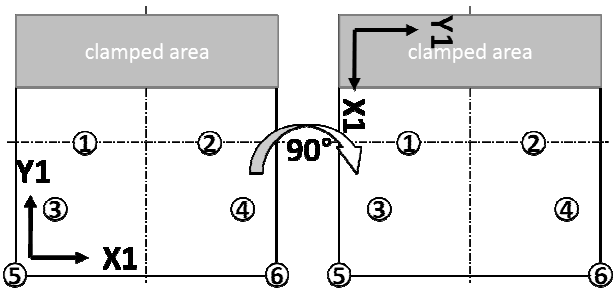

Fig. 7. Attachment types for determining direction-dependence (with same excitation point distribution for each direction)

Rys. 7. Sposoby mocowania w celu wyznaczenia kierunkowości (z takim samym rozmieszczeniem punktów wzbudzania w danym kierunku)

An exemplary result for the influence of fibre direction on FRF is shown in Figure 8 for AF-PP plate 2. Measurable changes (over the scattering) in modal parameters caused by fibre direction ΔMP_{FD} for all six AF-PP samples calculated from (2) are presented in Table 3 in the grey filled rows. The bold numbers mean shifts in the same directions (positive or negative) for all the examined plates. For the AF-PP plates, shifts in the same direction occur in natural frequencies of the 1st and 3rd mode. Obviously such changes could not be detected in the PET-UD/ISO - PP samples due to the smaller degree of anisotropy as shown in Figure 6.

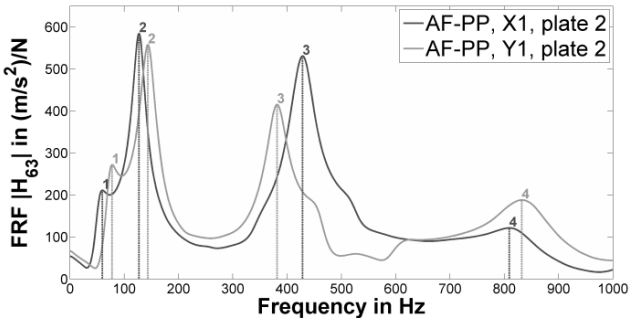

Fig. 8. Influence of fibre direction on FRF H_{63} (AF-PP plate 2)

Rys. 8. Wpływ ukierunkowania włókien na funkcję przejścia H_{63} (AF-PP plate 2)

$$\Delta MP_{FD} = MP_{X1} - MP_{Y1} \tag{2}$$

TABLE 3. **Changes in modal parameters caused by fibre direction**

TABELA 3. **Wpływ ukierunkowania włókien na parametry modalne**

mode	modal frequency [Hz]					
	plate 1	plate 2	plate 3	plate 4	plate 5	plate 6
1	**–21.5**	**–18.0**	**–18.2**	**–6.1**	**–22.9**	**–16.2**
2	–19.5	–16.4	–10.4	1.0	–11.3	–7.6
3	**67.6**	**46.9**	**53.7**	**69.7**	**47.3**	**40.6**
4	7.4	–23.0	–27.5	93.2	2.7	12.1
Mode	**Amplitude [(m/s²)/N]**					
	plate 1	**plate 2**	**plate 3**	**plate 4**	**plate 5**	**plate 6**
1	–104.8	–60.7	–166.7	24.7	–40.5	2.6
2	–529.9	26.7	–120.3	367.2	–39.2	–20.1
3	–136.4	115.4	90.6	179.2	111.1	16.2
4	109.5	–66.6	–107.6	–41.3	146.4	54.4
Mode	**Modal damping [%]**					
	plate 1	**plate 2**	**plate 3**	**plate 4**	**plate 5**	**plate 6**
1						
2	–26.83	0.68	1.37	21.58	–0.98	–0.94
3	–0.43	–0.14	0.17	2.73	1.62	0.50
4						

Instrumented free-falling dart method

The impact resistance of the samples was examined by the instrumented free-falling dart method by considering DIN EN ISO 6603-2:2000, according to all the setup parameters and conditions used in [2]. The char-

acteristic failure mode (high energy impact [8]) has got a maximum diameter of 40 mm on the bottom-side (see Fig 9). The results are presented in Figures 10 and 11.

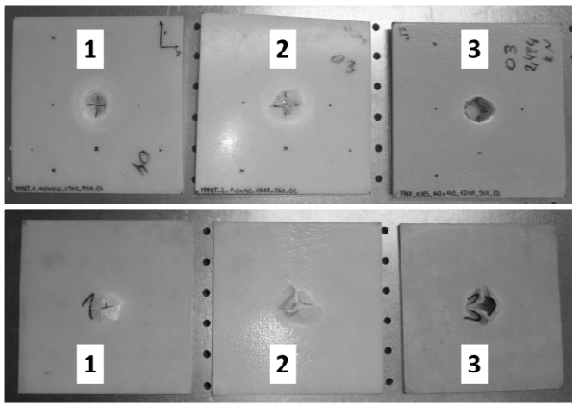

Fig. 9. Samples after drop-weight impact; bottom-side (lower); 1 - PET-UD-PP; 2 - PET-ISO-PP; 3 - AF-PP

Rys. 9. Próbki po przebiciu swobodnie spadającym grotem; spód (dolny); 1 - PET-UD-PP; 2 - PET-ISO-PP; 3 - AF-PP

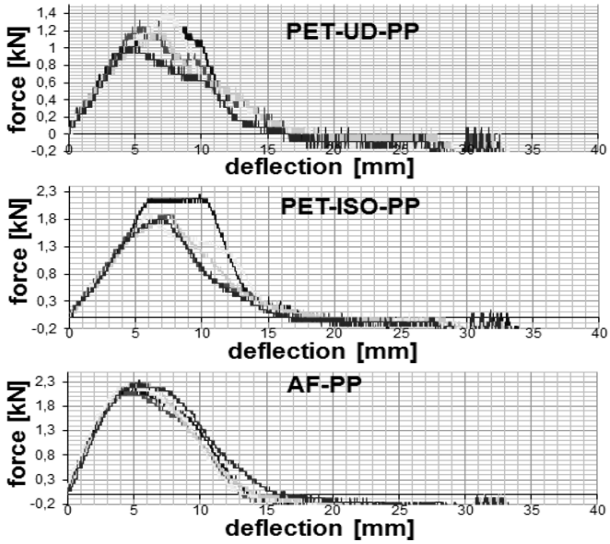

Fig. 10. Force-deflection graph free-falling dart method of all samples

Rys. 10. Wykres siła-ugięcie, instrumentalne badanie udarności dla wszystkich próbek

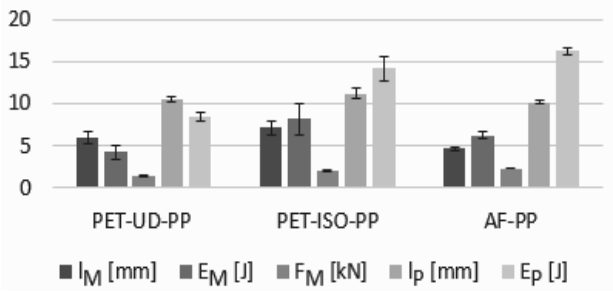

Fig. 11. Average value of instrumented free-falling dart method output parameters: l_M - deflection occurs at maximum force F_M; E_M - energy expended up to l_M; l_P - puncture deflection, when force dropped to half of F_M; E_P - energy expended up to l_P

Rys. 11. Zestawienie średnich wartości parametrów wyjściowych: l_M - ugięcie przy maksymalnej sile F_M; E_M - pomiar energii do wartości l_M; l_P - ugięcie przy przebiciu (spadku siły do połowy wartości F_M); E_P - energia zmierzona po przebiciu próbki do l_P

RESULTS AND DISCUSSION

Influence of impact damage on modal parameters

The results for changes after impact damage are presented in Figure 12 and Table 4 for FRF $|H_{63}|$.

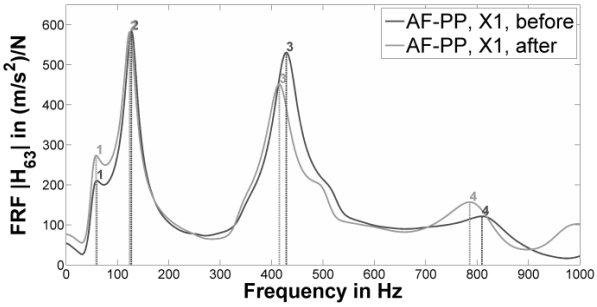

Fig. 11. Exemplary changes after impact damage in FRF

Rys. 11. Przykładowe zmiany w funkcji przejścia po przebiciu

$$\Delta MP_D = MP_{before} - MP_{after} \tag{3}$$

TABLE 4. **Changes after impact damage in modal parameters**
TABELA 4. **Zmiany w parametrach modalnych po przebiciu**

	m	plate 1		plate 2		plate 3		plate 4		plate 5	
		X1	Y1	X1	Y1	X1	Y1	X1	Y1	X1	Y1
PET-UD-PP	modal frequency [Hz]										
	1	3	–3	8	7	–3	0	30	0	–2	0
	2	29	–1	1	1	–5	7	–13	14	26	–1
	3	27	10	22	8	–4	–10	–26	6	–20	–47
	amplitude [(m/s²)/N]										
	1	93	–82	56	28	41	–88	230	–43	19	94
	2	–71	–139	13	6	–70	–76	–12	–110	–51	79
	3	–99	–99	2	–2	–80	–129	–140	–79	–32	43
	modal damping [%]										
	1	–3	2	–4	–12	0	1	–31	0	1	1
	2	3	4	2	0	2	–3	1	–4	24	0
	m	plate 1		plate 2		plate 3		plate 4		plate 6	
		X1	Y1	X1	Y1	X1	Y1	X1	Y1	X1	Y1
PET-ISO-PP	modal frequency [Hz]										
	1	1	2	3	–1	–3	–2	0	1	–2	–15
	2	–8	16	12	6	11	6	5	10	–16	–18
	3	–4	7	–29	15	–23	–32	–4	10	–21	–52
	amplitude [(m/s²)/N]										
	1	198	8	49	24	–3	–12	65	21	30	–272
	2	111	–22	76	–28	–37	0	43	39	–8	–162
	3	–116	–24	–64	–90	–49	–54	–65	–30	–23	–2
	modal damping [%]										
	1	–17	0	–1	0	–1	0	–3	1	1	19
	2	–8	–6	–45	–7	3	–2	–4	–12	3	10
	m	plate 1		plate 2		plate 3		plate 4		plate 6	
		X1	Y1	X1	Y1	X1	Y1	X1	Y1	X1	Y1
AF-PP	modal frequency [Hz]										
	1	4	7	–1	–1	–1	–4	1	3	0	0
	2	–16	–6	–3	0	1	–7	–7	2	1	1
	3	–33	–3	–14	1	–20	0	–15	–9	–6	5
	4	–49	–23	–24	–16	–42	–43	–26	–11	–20	20
	amplitude [(m/s²)/N]										
	1	33	50	62	15	30	–110	–33	31	–43	27
	2	–14	39	–2	82	4	–459	–37	385	6	–93
	3	–83	–19	–79	–10	–57	–85	–43	80	–19	10
	4	–105	–132	36	–9	10	6	–39	–118	–54	68
	modal damping [%]										
	2	1	–1	1	–1	0	19	0	–22	0	0
	3	1	0	0	1	0	2	1	–1	1	0

Table 4 shows shifts ΔMP_D in the modal parameters calculated from (3) between those of intact MP_{before} and damaged MP_{after} samples separately for X1 and Y1 directions. To examine an eventual loss of mass through the free-falling dart test, the samples were weighed before and after the test. The weight measuring accuracy of the used scale (KERN® Max. 220 g) was 0.1 mg. There was no loss in mass (max. 0.03%) after impact damage, only a local loss of stiffness. Measurable changes that lie above the scattering caused by the reattachment in natural frequencies, amplitudes ($|H_{63}|$) and modal damping are presented for all the samples in Table 4 in the grey filled rows.

Influence of perforation (open-hole) on modal parameters

Open-holes were produced in two samples (AF-PP plate 5 and PET-ISO-PP plate 5) using a drill machine, where the open hole was drilled over the centre position of the sample with a 20 mm diameter (see Fig. 12).

The examined plates show in both directions (X1, Y1) measurable changes in the FRFs as exemplary shown for AF-PP plate 5 in Figure 14.

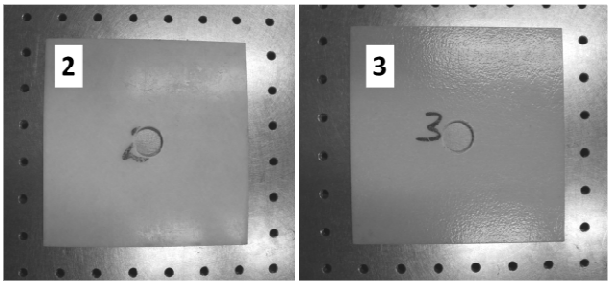

Fig. 12. Samples after hole drilling; 2 - PET-ISO-PP; 3 - AF-PP

Rys. 12. Próbki po wywierceniu otworów; 2 - PET-ISO-PP; 3 - AF-PP

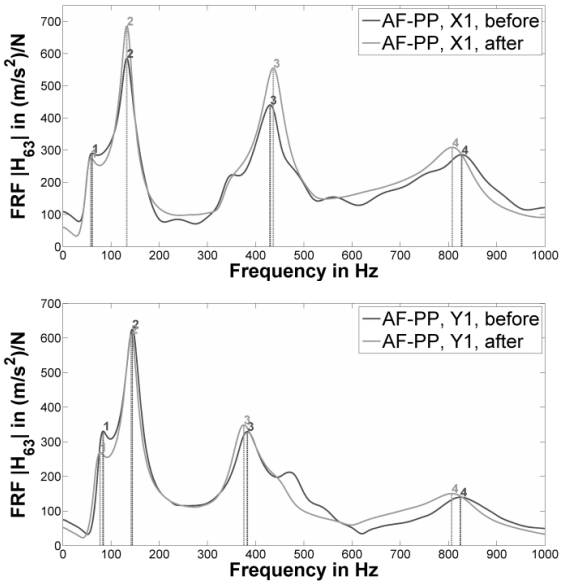

Fig. 13. FRFs in X1 (upper) and Y1 (lower) direction before and after hole drilling (AF-PP plate 5)

Rys. 13. Funkcje przejścia w kierunku X1 (górny) oraz Y1 (dolny) przed i po wywierceniu otworu (AF-PP plate 5)

The changes in modal parameters, presented in Table 5, were calculated as in the last section. Changes with the same sign occur for both plates in natural frequencies and modal damping.

TABLE 5. **Changes in modal parameters caused by open hole**
TABELA 5. **Zmiany w parametrach modalnych po wywierceniu**

	Mode	modal frequency [Hz]	
		X1	Y1
AF-PP plate 5	**1**	**–2.73**	**–6.45**
	2	0.0	–2.1
	3	6.4	–7.4
	4	**–19.53**	**–18.16**
	Mode	amplitude [(m/s²)/N]	
		X1	Y1
	1	–14.4	–61.2
	2	100.2	–14.8
	3	114.8	19.4
	4	22.6	10.5
	Mode	modal damping [%]	
		X1	Y1
	1	-	-
	2	**–2.2**	**–1.2**
	3	–0.5	0.5
	4	–1.4	1.8
PET-ISO-PP plate 5	Mode	modal frequency [Hz]	
		X1	Y1
	1	**1.4**	**3.5**
	2	**–14.1**	**–6.6**
	3	**17.4**	**5.5**
	Mode	amplitude [(m/s²)/N]	
		X1	Y1
	1	–3.1	95.3
	2	27.3	8.7
	3	–11.3	–36.4
	Mode	modal damping [%]	
		X1	Y1
	1	–0.6	–3.6
	2	**–13.3**	**–3.9**
	3	–0.8	–1.4

The samples were weighed before and after drilling. Table 6 shows the mass losses - which are very low but clearly detectable in changes in the modal parameters (local loss of stiffness and mass).

TABLE 6. **Masses of the samples before and after hole drilling**
TABELA 6. **Masy próbek przed i po wywierceniu otworu**

Sample	intact [g]	after drilling [g]	change [%]
PET-ISO-PP-05	57.57	56.62	–1.64
AF-PP-05	57.61	56.72	–1.54

CONCLUSIONS

Nonwoven (aramid and polyethylene terephthalate) thermoplastic (polypropylene) composite plates have been examined in terms of modal analysis based technical diagnostics. For this purpose, an appropriate fre-

quency band (0÷1 kHz) was determined for reproducible tests. A special device was built for the modal hammer that allowed a semi-automatic and significantly increase in the precision of excitation (max. 11.5-times better than by hand). Therefore in this work the semi-automatic excitation method was used to provide robust damage indicators (modal parameters).

A directionality study has been performed in which the orthotropic behavior of nonwoven composites could be detected in tensile tests and natural frequencies. These results can serve as a basis for a modal analysis based quality control system.

The influence of high energy impact and perforation (open hole) could also be undoubtedly detected in changes of the modal parameters. The examined samples with open holes show measurable changes even with the same sign in certain global modal parameters (natural frequencies and modal damping) that can be understood as a data pattern.

Acknowledgements

The source of funding the publication: "Federal Cluster of Excellence: Merge Technologies for Multifunctional Lightweight Structures" (DFG EXC 1075/1), "Innovativer regionaler Wachstumskern thermoPre® " (BMBF FK03WK CD4B) and "PT-Piesa" (DFG SFB/ TR 39).

REFERENCES

[1] Doebling S.W., Farrar C.R. Prime M.B., A Summary Review of Vibration-Based Damage Identification Methods, Los Alamos 1998.

[2] Nossol P., Czech A., Kroll L., Experimental investigation of dynamic behavior of thermoplastic fibre reinforced laminates, Composites Theory and Practice 2013, 2, 128-134.

[3] Albrecht W., Erth H., Fuchs H., Vliesstoffe: Rohstoffe, Herstellung, Anwendung, Eigenschaften, Prüfung, Wiley, 2012.

[4] Schürmann H., Konstruieren mit Faser-Kunststoff-Verbunden, 2. ed., Springer Verlag 2007.

[5] Schulze R., Heinrich M., Nossol P., Forke R., Sborikas M., Tsapkolenko A., Billep D., Wegener M., Kroll L., Gessner T., Piezoelectric P(VDF-TrFE) transducers assembled with micro injection molded polymers, Sensors and Actuators A: Physical 2014, 159-165.

[6] Kroll L., Elsner H., Heinrich M., Sticktechnologische Herstellung von Sensorstrukturen in textilen Trägermaterialien, Melliand Textilberichte: European Textile Journal 2008, Februar 26-27.

[7] Bond-Laminates GmbH, 15 Januar 2015. [Online]. Available: http://www.bond-laminates.com/en/tepexr-materials.html. [Accessed 15 January 2015].

[8] Matthews F.L., Damage in Fibre Reinforced Plastics; Its Nature, Consequences and Detection, Proceedings of the 3rd International Conference on Damage Assessment of Structures (DAMAS 99), 1999, 1-16.

